Direct Observation of Lattice Polaron Formation in the Local Structure of $La_{1-x}Ca_xMnO_3$

S. J. L. Billinge,[1] R. G. DiFrancesco,[1] G. H. Kwei,[2] J. J. Neumeier,[3] and J. D. Thompson[3]
[1]*Department of Physics and Astronomy and Center for Fundamental Materials Research, Michigan State University, East Lansing, Michigan 48824-1116*
[2]*Chemistry and Materials Sciences Department, Lawrence Livermore National Laboratory, Livermore, California 94550*
[3]*Los Alamos National Laboratory, Los Alamos, New Mexico 87545*
(Received 11 April 1996)

The local atomic structure of $La_{1-x}Ca_xMnO_3$ ($x = 0.12$, 0.21, and 0.25) has been studied using pair-distribution-function analysis of neutron powder-diffraction data. A change is seen in the local structure which can be correlated with the metal-insulator transition in the $x = 0.21$ and 0.25 samples. This local structural change is modeled as an isotropic collapse of oxygen towards Mn of magnitude $\delta = 0.12$ Å occurring on one in four Mn sites. We argue that this is the direct observation of lattice polaron formation, associated with the metal-insulator transition in these materials. [S0031-9007(96)00719-3]

PACS numbers: 71.30.+h, 61.12.–q, 71.38.+i, 72.80.Ga

The discovery in the 1950s of ferromagnetism coupled with a metal-insulator (MI) transition in the class of materials $La_{1-x}A_xMnO_3$, where A is a divalent ion [1], led to a theoretical explanation which involved a new type of exchange interaction called double exchange (DE) [2]. There has recently been a resurgence of interest in these materials for two reasons. First, a very large magnetoresistance, first observed by Volger [3], was rediscovered in thin films of $La_{0.67}Ba_{0.33}MnO_3$ [4], and also in a variety of thin films and bulk samples with similar chemical compositions [5,6]. This raises the possibility of using these materials in magnetic field sensors and magnetic read-write heads. Second, a question has been raised as to whether double exchange is the only physics governing the properties of these materials [7]. Millis *et al.* [7] argue that, to explain the experimental observations, an additional effect must be present to reduce the electron kinetic energy at the MI transition. A number of authors have proposed that it is a polaronic mechanism, either magnetic [6,8] or lattice [7,9,10] which is important. The presence of Jahn-Teller effects in these materials also is expected to enhance polaron formation [7,11]. It is clearly necessary to establish the presence of polarons experimentally and to characterize them. The presence of lattice polarons can be inferred indirectly from changes in refined thermal parameters [7]. However, except in the special cases where they are ordered over long range, a *local* structural probe is required to analyze them directly.

We have used the atomic-pair distribution function (PDF) analysis of neutron powder-diffraction data to study the *local* structure of $La_{1-x}Ca_xMnO_3$ for $x = 0.12, 0.21$, and 0.25 as a function of temperature. This enables us to look for a local structural response to the metal-insulator transition indicating the formation of randomly distributed lattice polarons. We recover experimentally the real-space pair correlation function which shows the relative positions of atoms in the structure as a function of distance. This approach has been shown to yield quantitative local-structural information as a function of distance in well-ordered materials [12,13] as well as in its traditional application to glasses and amorphous materials [14]. The approach has been described in detail elsewhere [12,15]. The temperature dependence of the local structure was studied as the samples went through the metal-insulator transition. We observe a local structural response to the MI transition which is evident as an abrupt broadening of certain PDF peaks. The two PDF peaks which are most strongly affected involve the nearest-neighbor Mn-O and O-O correlations. These bonds make up the MnO_6 octahedron. The abrupt changes in peak height are clearly seen in all the samples close to T_c^m, where T_c^m denotes the temperature of the combined ferromagnetic and metal-insulator transition, and they track T_c^m as it changes with composition x. There is no MI transition in the $x = 0.12$ sample, and we observe no corresponding structural change. Thus there is a clear correlation between the response of the local structure and the localization of carriers [16]. This indicates the formation of lattice polarons which are directly observed in the PDF. The polarons have been successfully modeled as a static breathing mode distortion of oxygen around manganese of magnitude $\delta \sim 0.12$ Å.

Powder samples were made by solid state reaction of La_2O_3, $CaCO_3$, and MnO_2 with repeated grindings and firings at temperatures up to 1400 °C, with a final slow cool at 1 °C per minute. The dc magnetization was measured using a commercial SQUID magnetometer and the temperature dependent resistivity was measured using the standard four-probe dc technique. Neutron powder-diffraction data were collected at the High Intensity Powder Diffractometer at the Manuel Lujan Jr. Neutron Scattering Center (MLNSC) at Los Alamos National Laboratory and at the Special Environment Powder Diffractometer at the Intense Pulsed Neutron Source (IPNS) at Argonne National Laboratory. Samples of around 10 g were sealed in a

cylindrical vanadium tube with He exchange gas. Data were collected as a function of temperature, concentrating on the region around T_c^m, using a closed cycle He refrigerator. Data collection and analysis procedures have been described elsewhere [12]. The powder-diffraction data are corrected for background, absorption, multiple scattering, and inelasticity effects, and are normalized by the incident flux and the number of scatterers. The resulting structure function $S(Q)$ is Fourier transformed to obtain $G(r)$, the atomic pair correlation function.

Examples of the transformed data are shown in Fig. 1. Two data sets are shown to illustrate the level of reproducibility of the data. They are from the $La_{0.88}Ca_{0.12}MnO_3$ sample at 150 and 180 K. This sample has no metal-insulator transition and is not undergoing a structural change in this temperature range, as we will discuss. The difference curve $\Delta = G(150\ \mathrm{K}) - G(180\ \mathrm{K})$ is plotted below the PDFs. The dotted lines show the expected uncertainties in the difference due to statistical fluctuations at the level of two standard deviations. It is clear that the experimental PDFs are obtained as a function of temperature with high reproducibility and the observed fluctuations are at the level of the statistical uncertainties.

To look for possible local structural changes with temperature we examine the temperature dependence of the peak height of the PDF peak located at $r = 2.75$ Å, shown in Fig. 2. This is a strong positive peak (see Fig. 1) which originates from the O-O atomic pairs which make up the MnO_6 octahedron. The integrated area under a PDF peak is a measure of the multiplicity of the atom-pair correlation giving rise to the peak and does not change with temperature. Thus we can use the PDF peak height as a sensitive measure of the *width* of the correlation which gives the *distribution* of atomic distances. An abrupt change in the peak height indicates a change in the degree of order of the underlying correlation. By considering the peak at $r = 2.75$ Å, we focus on the behavior of the MnO_6 octahedron independently of the rest of the structure. The bonding in this octahedron is an important indicator of polaron formation on the Mn site.

The three panels in Fig. 2 show data from three samples: (a) $x = 0.25$, (b) $x = 0.21$, and (c) $x = 0.12$. The measured resistivities of these samples are shown in the insets. The MI transition temperature, defined as the maximum in $\rho(T)$, is indicated by an arrow in the insets, and also on the main plots. The solid lines in the figure

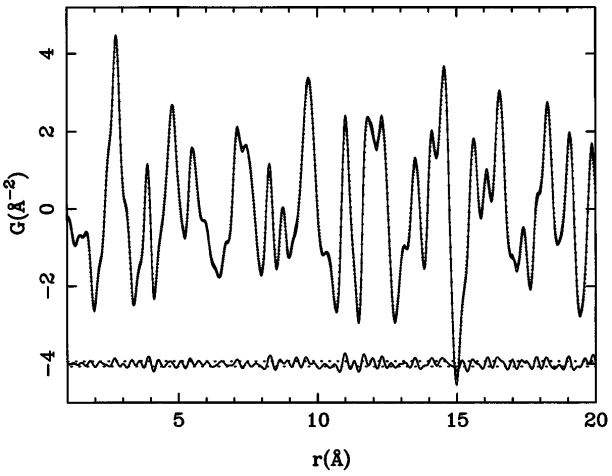

FIG. 1. PDFs obtained from the $La_{0.88}Ca_{0.12}MnO_3$ sample. The solid line shows the PDF collected at 150 K and the dashed line at 180 K. The difference curve $\Delta = G(150\ \mathrm{K}) - G(180\ \mathrm{K})$ is plotted below the data. The dashed lines on the difference curve indicate the expected fluctuations, based on the counting statistics of the data, at the level of two standard deviations. The data reproduce at the level of the expected fluctuations, which demonstrates the reproducibility that can be expected from the experimental PDFs.

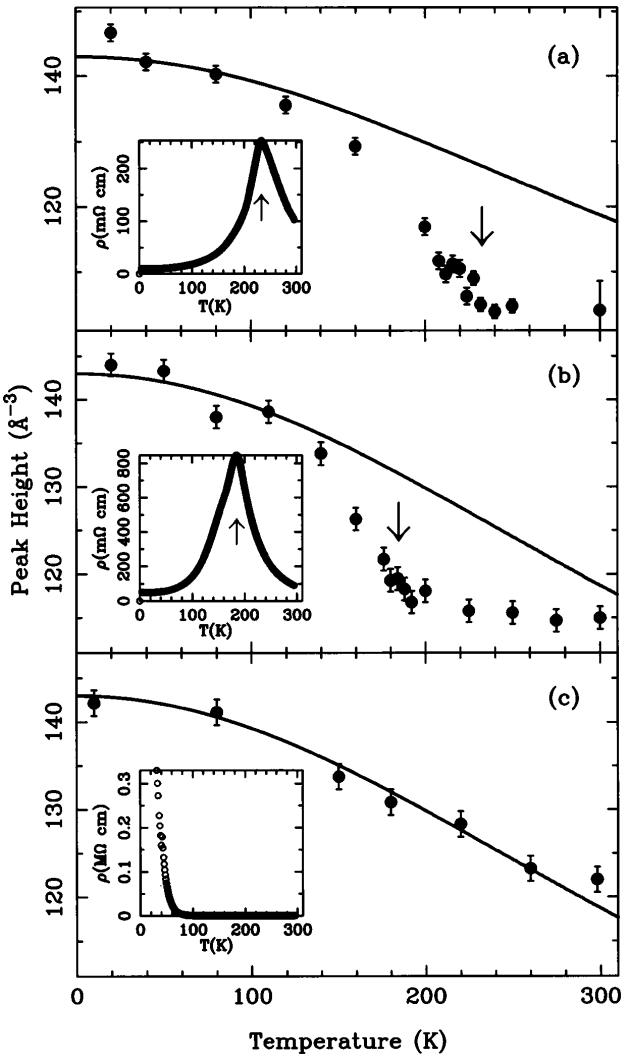

FIG. 2. Height of the PDF peak at $r = 2.75$ Å vs temperature for various values of x. (a) $x = 0.25$, (b) $x = 0.21$, and (c) $x = 0.12$. The insets show resistivity vs temperature for the same samples. The arrows indicate the MI transition temperature in the insets and the main panels.

indicate the expected evolution of the peak height with temperature. As the temperature rises, the PDF peaks broaden and the peak height falls due to increases in the mean-square amplitude of thermal motion, $\langle u^2 \rangle$. The expected temperature dependence is calculated using the Debye expression for $\langle u^2 \rangle$ with two fitting parameters: the peak height at $T = 0$, h_0, and the Debye temperature Θ_D. The peak heights in Fig. 2 have been rescaled so that h_0 is the same for each sample and the same Debye-Waller curve is plotted in each panel.

The $x = 0.12$ sample has no MI transition and remains insulating to low temperatures. The temperature dependence of its PDF peak at $r = 2.75$ Å is well explained by thermal motions: There is no underlying change in the local structure. However, all of the samples which exhibit a MI transition have an abrupt change in peak height close to T_c^m indicating a non-Debye-like change in the local structure. The peak height is lower, the peaks broader, and therefore a larger distribution of O-O bond lengths is evident in the paramagnetic insulating (PI) phase. Similar behavior to that shown in Fig. 2 is evident in the negative PDF peak at 1.9 Å, which originates from the Mn-O nearest-neighbor distance. This suggests that the distortion of the octahedron is driven by changes in the Mn-O bond-length distribution. Other peaks, such as the negative Mn-La/Ca peak at 3.4 Å, do not show the abrupt changes at T_c^m since they are not sensitive to distortions of the octahedron. This result is in qualitative agreement with various crystallographic [17] and local structure studies [18] which suggest an increase in the oxygen Debye-Waller factor associated with T_c^m.

The change in the PDF peak height at the MI transition has a natural explanation in terms of lattice polaron formation. The qualitative behavior of the PDF can be understood by considering the two limiting cases of delocalized and localized charge carriers (holes). If the carriers are completely delocalized, the carrier charge density is evenly distributed among the Mn sites and there are no distinct Mn^{3+} and Mn^{4+} ions. An average distortion to the octahedron will exist but there will be well-defined Mn-O bond lengths which are fully ordered. In the other extreme we can assume that the holes on the Mn^{4+} ions become localized as small polarons. Now there are two distinct kinds of ions with their own preferred bonding environment. We expect the *average* bond length to be the same as in the previous case (ignoring other long-range effects such as magnetostriction, etc.), but the *local bond length* will take on different values depending on whether the local Mn ion has a 3+ or a 4+ charge. This is exactly what is seen in the data. In the low temperature metallic phase the bond distribution is sharp. As the MI transition is approached from below, the correlations broaden indicating the distribution of Mn-O bond lengths is increasing consistent with the formation of small polarons. This behavior saturates close to T_c^m, at which point the polarons are fully formed. This is consistent with transport measurements in the PI phase which are well explained by a small polaron hopping mechanism [19].

It is interesting to note from Fig. 2 that the atomic correlations begin to broaden below T_c^m. The local structure is beginning to disorder while the sample is still metallic. It is possible that the polarons are large, spread over more than one atomic site, and dynamic in this region. This might be consistent with the observation of Hundley *et al.* [19] that the resistivity can also be modeled as polaronic in the region immediately below the T_c^m. Alternatively, microscopic inhomogeneities in the sample, for instance, due to the presence of the Ca doping ions or La vacancies, may allow some carriers to localize and become trapped at a lower temperature while the sample as a whole is still metallic.

To investigate the nature of the local structural change at T_c^m, we have calculated the effect on the PDF of introducing local breathing-mode type distortions to the MnO_6 octahedra. The model we used for the polaronic lattice distortion is described below. Note that at these compositions, the static *average* Jahn-Teller (JT) distortion of the MnO_6, obtained from the crystal structure, is very small ($r_{\text{Mn-O}}^{\max} - r_{\text{Mn-O}}^{\min} < 0.05$ Å). Displacements of oxygen which simply destroy these average JT distortions and make the octahedron of the Mn^{4+} ion undistorted are too small to explain the observed change in the PDF. We consider for the polaronic lattice distortion a uniform contraction of the six Mn-O bonds on the affected Mn site, consistent with an isotropic collapse of the oxygen octahedron around the highly charged 4+ ion. The results are shown in Fig. 3. The upper set of curves (i) in Fig. 3(a) shows the appearance in the *data* of the structure change at T_c^m. The PDFs are from the $x = 0.21$ sample at $T = 140$ K (solid line) and 176 K (dotted line). Although the changes in the PDFs are small, they are significant. This can be seen by a careful comparison of the upper set of curves in Fig. 3(a) (i), where structural changes are evident, with Fig. 1 which shows two data sets collected over a similar temperature range but from the $x = 0.12$ sample which has no underlying structural change.

The effect on the PDF of introducing the polaronic distortion into the model is shown in the lower set of curves (ii) in Fig. 3(a). The solid line is the PDF from the model without the distortion and the dotted line the model with the distortion described above with $\delta = 0.12$ Å. To better see how successful the model is at explaining the structural changes in the data, in Fig. 3(b) we show the *difference curves* from the PDFs shown in Fig. 3(a). The circles show the changes in the data on warming from below to above T_c^m. The solid line shows the changes in the model PDF due to the introduction of the polaronic distortion described above. The changes in the data at T_c^m are well matched by the changes in the model on introducing the polaron. The largest changes in the data,

for example, at $r = 2$, 2.8, 8.3, and 10 Å in the difference curves, are well reproduced by the modeled distortion. Such self-consistent agreement over a wide range of r is strong evidence that the main features of the model are correct. However, the experimental difference curve is not fully reproduced, and it is unlikely that this simple model is correct in every detail.

In conclusion, we have observed directly for the first time the formation of small lattice polarons in the local structure of $La_{1-x}Ca_xMnO_3$ using the pair distribution function analysis of neutron powder-diffraction data. The polaronic distortion of the lattice is well modeled as a uniform collapse of the MnO_6 octahedron associated with the Mn^{4+} site. The oxygen displacements of the distortion are $\delta = 0.12$ Å when it is assumed that a hole localizes on one in four of the Mn sites. The polaron formation is closely associated with the MI transition, although PDF peak broadening begins below T_c^m suggesting precursor effects to the charge localization.

We are grateful to A. R. Bishop, T. Egami, M. F. Hundley, and A. J. Millis for useful discussions. S. J. B. would like to thank the Alfred P. Sloan Foundation for support as a Research Fellow. The IPNS is funded by U.S. DOE under Contract No. W-31-109-ENG-38 and the MLNSC is a national user facility funded by DOE-BES and DOE-DP. Work at Livermore and Los Alamos was performed under the auspices of the DOE under Contracts No. W-7405-ENG-48 and No. W-7405-ENG-36, respectively.

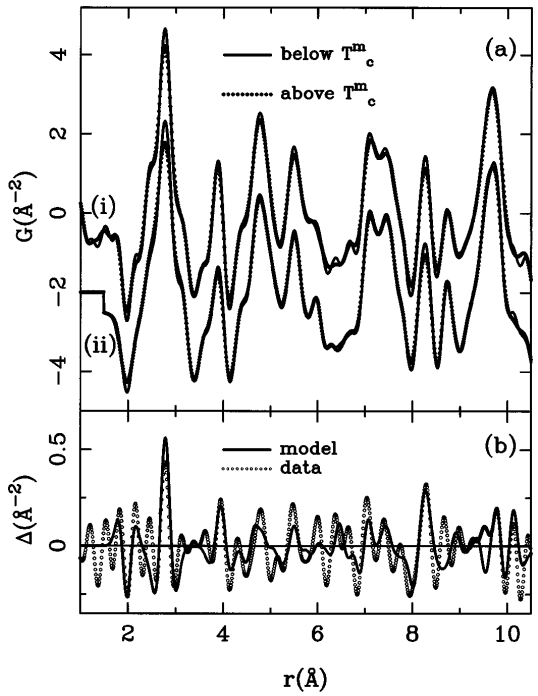

FIG. 3. (a) Comparison of the change observed in the data on going through T_c^m [curves (i)] with the change produced in the model PDF by introducing a polaronic distortion (described in the text) [curves (ii)]. In both (i) and (ii), the solid line represents the PDF below the structure change at T_c^m with no polaron present and the dotted line the PDF above this temperature with polaronic distortions present. (b) shows the difference curves from the curves in (a). Circles show the changes in the data PDF [(a) (i)] and the solid line the changes in the model PDF [(a) (ii)].

[1] G. M. Jonker and J. H. van Santen, Physica (Utrecht) **16**, 337 (1950); E. O. Wollan and W. F. Koehler, Phys. Rev. **100**, 545 (1955); C. W. Searle and S. T. Wang, Can. J. Phys. **47**, 2703 (1969); **48**, 2023 (1970).
[2] C. Zener, Phys. Rev. **82**, 403 (1951); P. W. Anderson and H. Hasegawa, Phys. Rev. **100**, 675 (1955); P. G. de Gennes, Phys. Rev. **118**, 141 (1960); K. Kubo and A. Ohata, J. Phys. Soc. Jpn. **33**, 21 (1972).
[3] J. Volger, Physica (Utrecht) **20**, 49 (1954).
[4] R. von Helmolt *et al.*, Phys. Rev. Lett. **71**, 2331 (1993).
[5] H. L. Ju *et al.*, Appl. Phys. Lett. **65**, 2108 (1994); K. Cahara, T. Ohno, M. Kasai, and Y. Kozono, Appl. Phys. Lett. **63**, 1990 (1993); R. Mahendiran *et al.*, Appl. Phys. Lett. **66**, 233 (1995).
[6] R. M. Kuster, D. A. Singleton, R. McGreevey, and W. Hayes, Physica (Amsterdam) **155B**, 362 (1989).
[7] A. J. Millis, P. B. Littlewood, and B. I. Shraiman, Phys. Rev. Lett. **74**, 5144 (1995).
[8] J. M. D. Coey, M. Viret, L. Ranno, and K. Ounadjeda, Phys. Rev. Lett. **75**, 3910 (1995).
[9] H. Röder, J. Zang, and A. R. Bishop, Phys. Rev. Lett. **76**, 1356 (1996).
[10] Y. X. Jia *et al.*, Phys. Rev. B **52**, 9147 (1995).
[11] A. J. Millis, Phys. Rev. B **53**, 8434 (1996).
[12] S. J. L. Billinge and T. Egami, Phys. Rev. B **47**, 14 386 (1993).
[13] S. J. L. Billinge, G. H. Kwei, and H. Takagi, Phys. Rev. Lett. **72**, 2282 (1994).
[14] A. C. Wright *et al.*, in *Neutron Scattering for Materials Science II*, edited by D. A. Neumann, T. P. Russell, and B. J. Wuensch, MRS Symposia Proceedings No. 376 (Materials Research Society, Pittsburgh, 1995), p. 635.
[15] T. Egami, Mater. Trans. JIM **31**, 163 (1990).
[16] The structure change correlates with the MI transition and not with the appearance of ferromagnetism. This is clear since the $x = 0.12$ sample becomes ferromagnetic at a T_c of $\approx$165 K, with an ordered moment which is comparable to that observed in the other composition samples, although it remains insulating to the lowest temperatures. If the PDF were sensitive to the ferromagnetism rather than the structure change associated with the MI transition, it would be evident in the $x = 0.12$ sample and it is not (Fig. 1).
[17] P. G. Radaelli *et al.* (unpublished); G. H. Kwei, S. J. L. Billinge, R. G. DiFrancesco, and J. J. Neumeier (unpublished); D. N. Argyriou *et al.*, Phys. Rev. Lett. **76**, 3826 (1996).
[18] T. A. Tyson *et al.* (unpublished); D. Louca *et al.* (unpublished).
[19] M. F. Hundley *et al.*, Appl. Phys. Lett. **67**, 860 (1995).